

Novel Ultrabright Luminescent Copper Nanoclusters and Application in Light-Emitting Devices

*Qiu-Qin Huang,^a Mei-Yue Hu,^a Yan-Li Li,^a Nan-Nan Chen,^a Yi Li,^a Qiao-Hua Wei^{*a,b}
and FengFu Fu^{*a}*

^a MOE Key Laboratory for Analytical Science of Food Safety and Biology, Fujian Provincial Key Laboratory of Analysis and Detection Technology for Food Safety, Fujian Provincial Key Laboratory of Electrochemical Energy Storage Materials, College of Chemistry, Fuzhou University, Fuzhou, Fujian 350108, China.

^b State Key Laboratory of Structural Chemistry, Fujian Institute of Research on the Structure of Matter and Graduate School of CAS, Fuzhou, Fujian 350002, China.

E-mail: qhw76@fzu.edu.cn, fengfu@fzu.edu.cn.

Table of Contents

content	page
Cover page	1
Table of Contents	2
Experimental Section	3
Fabrication of LEDs	4
Crystal Structural Determination	5
Calculation Detail	6
Characterizations (Fig. S1-S4)	7-10
Crystal Structures (Fig. S5, Table S1-S2)	11-13
Photophysical Properties (Table S3, Fig. S6)	14-15
Performance Comparison (Table S4)	16
References	17

Experimental Section

Materials and Reagents. Copper(II) perchlorate hexahydrate($\text{Cu}(\text{ClO}_4)_2 \cdot 6\text{H}_2\text{O}$, 98%), sodium borohydride (NaBH_4 , 96%), copper powder, were purchased from commercial sources without further purification. $[\text{Cu}(\text{MeCN})_4]\text{ClO}_4$ and $[\text{Cu}_2(\text{dppy})_3(\text{MeCN})](\text{ClO}_4)_2$ were prepared by previous report.¹

General methods

NMR spectra were measured in CD_2Cl_2 on a Bruker AVANCE 400 spectrometer. The mass spectra were obtained with an ESI-TOF-MS spectrometer DECAX-3000 LCQ Deca XP. The morphology of samples was determined by transmission electron microscopy (TEM) and high resolution transmission electron microscopy (HRTEM) analysis (Tecnai G2 F20 instrument FEI, USA). X-ray crystallographic analyses were recorded on a D8 Venture by using $\text{Mo K}\alpha$ radiation. FT-IR spectra were recorded on a BRUKER-EQUINOX-55 IR spectrophotometer and XPS spectra were analyzed using ESCALAB 250Xi to confirm the chemical composition of samples. Thermogravimetric analysis (TGA) was characterized on TG209F1 by heating the samples in air up to 800°C with a heating rate of 5°C min^{-1} . Steady-state photoluminescence spectra and quantum yield (Φ) of the samples were obtained using a Edinburgh FS5 spectrofluorometer with a 150W Xenon lamp. The Φ values of samples were measured with a 6-inch integrating sphere using single photon counting mode. Time-resolved photoluminescence decay curves were obtained using a FLS920 Fluorescence Spectrometer equipped with a microsecond flash-lamp (μF900).

Synthesis

Synthesis of $[\text{Cu}_3\text{H}(\text{dppy})_4](\text{ClO}_4)_2$ (1) and $[\text{Cu}_4\text{H}(\text{dppy})_4\text{Cl}_2](\text{ClO}_4)$ (2)

The CH_3OH solution containing NaBH_4 (22.7 mg, 0.6 mmol) was added to the solution of $[\text{Cu}_2(\text{dppy})_3(\text{MeCN})](\text{ClO}_4)_2$ (236 mg, 0.2 mmol) in 2 mL CH_2Cl_2 and 4 mL CH_3OH . The mixture was stirred for two hours at room temperature from colorless clear solution changed to orange red clear solution. Then, the solvent was removed and re-dissolved with CH_2Cl_2 to remove excess NaBH_4 . Yellow cubic crystals **1** and yellow green acicular crystals **2** were obtained by recrystallization using MeOH / diethyl ether and $\text{ClCH}_2\text{CH}_2\text{Cl}$ / diethyl ether, respectively.

1: Yield: 75.6 mg (39.4 %, calculated by the content of Cu). ^1H NMR (400 MHz, CD_2Cl_2 , δ , ppm): 7.94 (t, $J = 16.0$ Hz, 4H), 7.77 (s, 4 H), 7.54-7.48 (m, 12H), 7.31-7.23 (m, 20H), 7.07-7.03 (t, 16H). $^{31}\text{P}\{^1\text{H}\}$ NMR (400MHz, CD_2Cl_2 , δ , ppm): 7.06 (s). ESI-MS [m/z (%): 622.07 (100 %) $[\text{Cu}_3\text{H}(\text{dppy})_3]^{2+}$, 1080.00 (5 %) $\{[\text{Cu}_3\text{H}(\text{dppy})_3](\text{ClO}_4)\}^+$.

2: Yield: 62.7 mg (43.6 %, calculated by the content of Cu). ^1H NMR (400 MHz, CD_2Cl_2 , δ , ppm): 7.95 (t, $J = 16.0$ Hz, 4H), 7.77(s, 4 H), 7.54-7.48 (m, 12H), 7.32-7.25 (m, 20H), 7.05 (s, 16H). $^{31}\text{P}\{^1\text{H}\}$ NMR (400MHz, CD_2Cl_2 , δ , ppm): 7.43 (s). ESI-MS [m/z (%): 1379.01 (60 %) $[\text{Cu}_4\text{H}(\text{dppy})_4\text{Cl}_2]^+$, 1115.91 (65 %) $[\text{Cu}_4\text{H}(\text{dppy})_3\text{Cl}_2]^+$, 622.07 (100 %) $[\text{Cu}_3\text{H}(\text{dppy})_3]^{2+}$.

Fabrication of LEDs

The light-emitting diodes (LEDs) used for the electroluminescence (EL) was supplied by Shenzhen Chundaxin Optoelectronic Corp. The different loading amounts (6% or 3%) of cluster **1** were first mixed with stoichiometric pouring sealant (HN3153-TCA/B) and then stirred for 10 min. The mixture was deposited on top of the LED chip. It consists of a fully packaged Epileds InGaN LED Chips with an emission centered at 450 nm. The device was cured in an oven at 60 °C for 2 h to fabricate the yellow or white LEDs.

The initial LED chip was characterized with CIE, color rendering index (CRI), correlated color temperature (CCT), and luminance efficiency (LE) of (0.15, 0.03), -44.1, 100000 K, and 17.55 lm/W, respectively.

Crystal Structural Determination

The Crystal **1** and **2** coated with epoxy resin was measured on a Mar CCD 165 nm diffractometer by the oscillation scan technique at 173 K using monochromatic Mo K α radiation ($\lambda = 0.71073$ Å) under a cold nitrogen stream. The data were processed with CrysAlisPro 1.171.39.3a (Rigaku OD, 2015). The structure was solved by direct methods using the *SHELXS97* program and was refined by full matrix least-squares on F^2 using the program *SHELXL97*.² The positions of the nonhydrogen atoms were refined with anisotropic displacement factors. The hydrogen atoms were positioned geometrically by using a riding model. The distributions from vacancy of the crystal were hardly to refine using conventional discrete-atom models. To resolve these issues, the contribution of the electron density by the remaining free solvent of **2** was removed by the SQUEEZE routine in PLATON. The crystallographic parameters and details for data collections and refinements are summarized in Table S1, and the selected bond distances and angles are listed in Table S2. Full crystallographic data are also provided there as CIF files.

Calculation detail

The positions of the hydrides in **1** and **2** were corroborated by DFT calculations. All spin-polarized DFT calculations were performed using the Vienna ab initio simulation package (VASP) with the Projector Augmented Wave (PAW) method.^{3, 4} The generalized gradient approximation (GGA) with the Perdew-Burke-Ernzerhof (PBE) of the exchange-correlation functional was utilized. A plane-wave cutoff energy was set to 400 eV. The Γ point was used to sample the Brillouin zone integration. Electronic and ionic relaxations were performed until energies and maximum forces converged below 10^{-5} and 0.03 eV/Å, respectively. And the effects of van der Waals interactions were considered by using the dispersion-corrected vdW-DF2 functional.⁵

Characterizations

ESI-MS Analysis

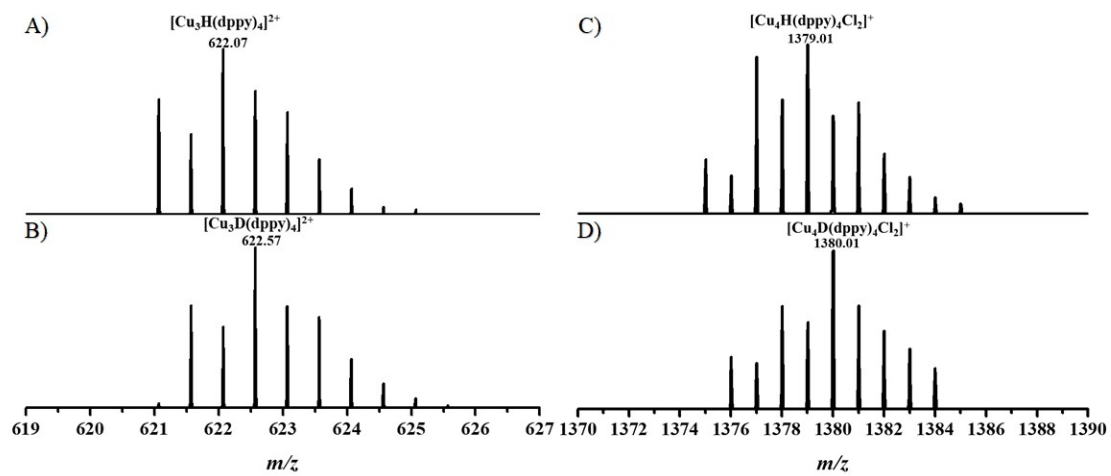


Fig. S1. ESI-TOF-MS spectra of 1^{2+} (A), 1_D^{2+} (B), and 2^+ (C), 2_D^+ (D).

Characterizations

TEM and HRTEM Analysis

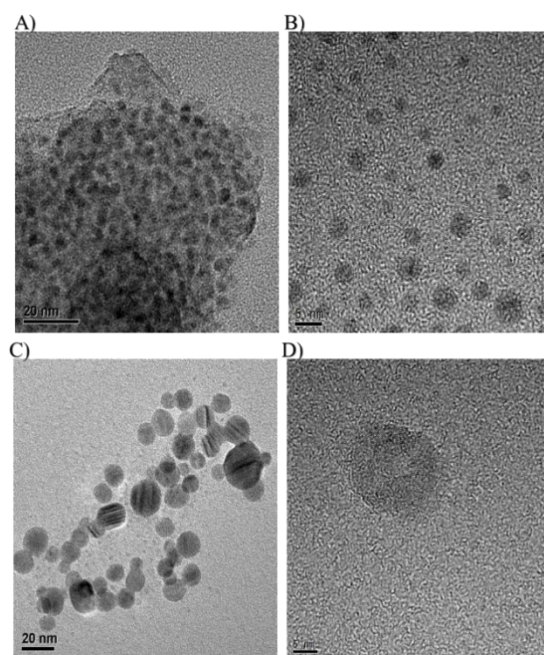


Fig. S2. TEM and HRTEM images of nanoclusters **1** (A, B) and **2** (C, D)

Characterizations

IR Analysis

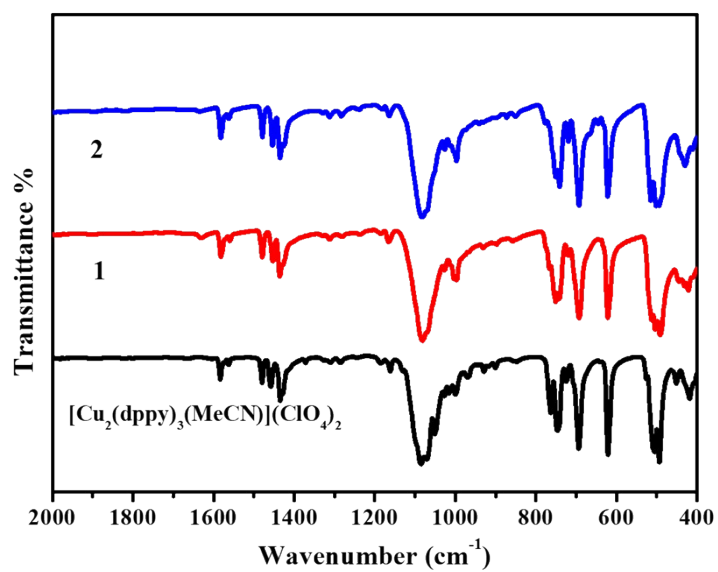


Fig. S3. IR spectra of $[\text{Cu}_2(\text{dppy})_3(\text{MeCN})](\text{ClO}_4)_2$, **1**, and **2**.

Characterizations

XPS Analysis

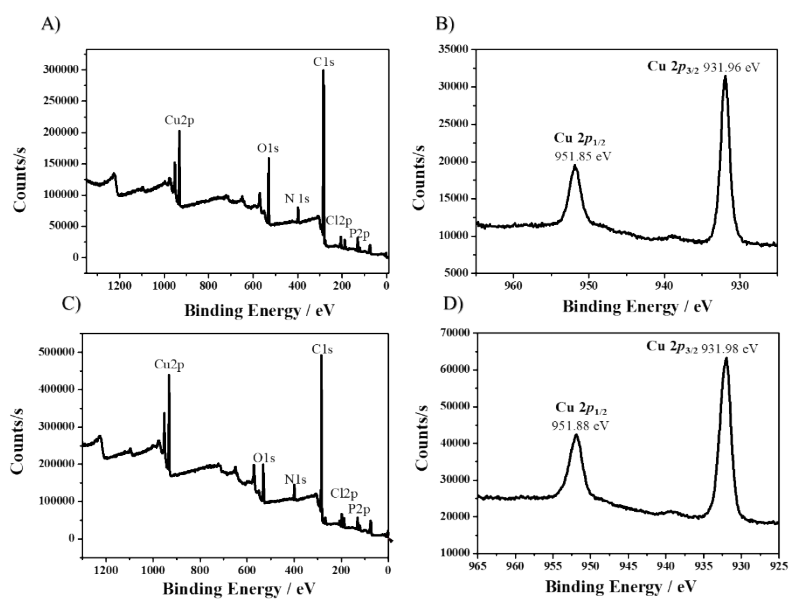


Fig. S4. XPS full-scan spectrum of nanocluster **1** (A), **2**(C), and Cu 2p spectrum of nanocluster **1** (B) and **2** (D).

Crystal Structures

DFT optimized structures

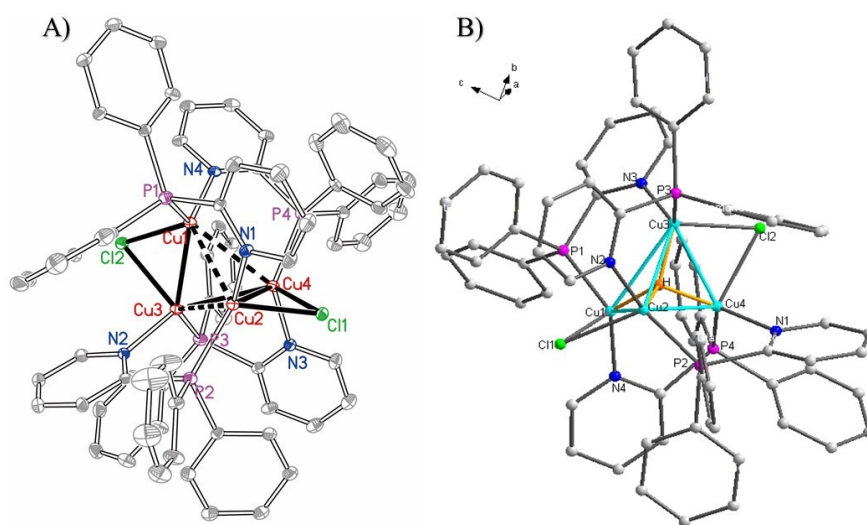


Fig. S5. ORTEP drawings (A) and DFT optimized structure (B) of 2^+ showing 30% thermal ellipsoids, and the hydrogen atoms on dppp ligands are omitted for the sake of clarity.

Crystal Structures

Table S1: Crystallographic data for clusters **1** and **2**.

Cluster	1 ·2CH ₂ Cl ₂ ·CH ₃ OH	2 ·ClCH ₂ CH ₂ Cl
Empirical formula	C ₇₁ H ₆₀ Cl ₆ Cu ₃ N ₄ O ₉ P ₄	C ₇₀ H ₆₀ Cl ₅ Cu ₄ N ₄ O ₄ P ₄
Formula weight	1640.43	1576.51
Temperature(K)	173(2)	293(2)
Wavelength (Å)	0.71073	0.71073
Crystal system	Monoclinic	Triclinic
space group	C2/c	P-1
<i>a</i> (Å)	49.294(3)	14.0903(5)
<i>b</i> (Å)	12.7809(6)	14.7705(4)
<i>c</i> (Å)	23.0005(13)	17.8312(7)
α (°)	90	72.082(3)
β (°)	98.205(4)	84.734(3)
γ (°)	90	88.356(3)
Volume (Å ³)	14342.4(13)	3516.1(2)
Z	8	2
ρ_{calcd} , g/cm ³	1.487	1.489
μ , mm ⁻¹	1.216	1.524
F(000)	0.0682	0.0429,
θ (°)	0.1954	0.1291
Limiting indices	-58<= <i>h</i> <=58, -15<= <i>k</i> <=14, -27<= <i>l</i> <=23	-16<= <i>h</i> <=16, -17<= <i>k</i> <=17, -21<= <i>l</i> <=18
Reflections collected/unique	49995 / 12613	25450 / 11869
R (int)	0.0544	0.0299
Goodness-of-fit on F ²	1.067	1.153
R1 (F _o)	0.0682	0.0429,
wR2(F _o ²)	0.1954	0.1291
Largest diff. peak and hole	3.197 and -1.079 (e·Å ⁻³)	1.129 and -1.183 (e·Å ⁻³)

Crystal Structures

Table S2: Selected bond distances (Å) and angles (°) for **1** and **2**.

	Bond distance [Å]			
	1		2	
Cu-Cu	Cu(2)-Cu(1) 2.7225 (11)		Cu(1)-Cu(4) 2.7222 (6)	Cu(2)-Cu(3) 2.9147 (6)
	Cu(3)-Cu(2) 2.7010 (10)		Cu(1)-Cu(2) 2.7425 (6)	Cu(2)-Cu(4) 2.9822 (6)
	Cu(3)-Cu(1) 2.7488 (11)		Cu(1)-Cu(3) 2.9814 (6)	Cu(3)-Cu(4) 2.5999 (6)
Cu-P	Cu(3)-P(4) 2.2636 (17)		Cu(1)-P(1) 2.2318 (10)	Cu(3)-P(3) 2.2187 (10)
	Cu(3)-P(2) 2.2832 (17)		Cu(2)-P(2) 2.2459 (10)	Cu(4)-P(4) 2.2130 (10)
	Cu(2)-P(3) 2.2602 (16)			
	Cu(2)-P(1) 2.2752 (18)			
Cu-N	Cu(3)-N(1) 2.101 (5)		Cu(1)-N(4) 2.078 (3)	Cu(3)-N(2) 2.066 (3)
	Cu(2)-N(2) 2.101 (5)		Cu(2)-N(1) 2.095 (3)	Cu(4)-N(3) 2.063 (3)
	Cu(1)-N(3) 1.986 (5)			
	Cu(1)-N(4) 2.029 (6)			
Cu-Cl			Cu(1)-Cl(1) 2.4378 (10)	Cu(3)-Cl(2) 2.4082 (10)
			Cu(2)-Cl(1) 2.4100 (10)	Cu(4)-Cl(2) 2.4088 (10)
	Bond angles [°]			
P-Cu-P	P(4)-Cu(3)-P(2)	122.40 (6)		
	P(3)-Cu(2)-P(1)	122.34 (7)		
N-Cu-N	N(3)-Cu(1)-N(4)	126.0 (2)		
N-Cu-P	N(1)-Cu(3)-P(4)	110.62 (15)	N(4)-Cu(1)-P(1)	120.06 (9)
	N(1)-Cu(3)-P(2)	102.55 (15)	N(1)-Cu(2)-P(2)	123.30 (9)
	N(2)-Cu(2)-P(3)	113.14 (14)	N(2)-Cu(3)-P(3)	118.97 (9)
	N(2)-Cu(2)-P(1)	101.46 (15)	N(3)-Cu(4)-P(4)	111.15 (9)

Photophysical Properties

Table S3: Photophysical data of **1** and **2** in different solvents and solid states.

NCs	medium	$\lambda_{\text{abs}} / \text{nm}$	$\lambda_{\text{em}} / \text{nm}$	$\Phi / \%$
		$(\epsilon \times 10^4 / \text{dm}^3 \cdot \text{mol}^{-1} \cdot \text{cm}^{-1})$	$(\tau_{\text{em}} / \mu\text{s})$ (298K)	
1	Solid		553(9.0)	71.8
	ClCH ₂ CH ₂ Cl	224 (0.41), 260 (0.19), 320 (0.08), 385 (0.02)	577	0.13
	CH ₂ Cl ₂	228 (0.60), 270 (0.31), 320 (0.15), 390 (0.04)	585	0.11
	MeOH	206 (0.79), 255 (0.23), 390 (0.02)	600	0.39
	MeCN	205 (1.11), 255 (0.29), 325 (0.06), 388 (0.01)	643	0.24
2	Solid		543(4.2)	63.5
	ClCH ₂ CH ₂ Cl	225 (0.70), 260 (0.33), 310 (0.17), 380 (0.03)	568	<0.01
	CH ₂ Cl ₂	227 (0.68), 260 (0.38), 310 (0.23), 380 (0.04)	565	0.93
	MeOH	207 (1.08), 260 (0.35), 310 (0.21), 380 (0.04)	570	0.71
	MeCN	207 (1.32), 260 (0.34), 310 (0.19), 380 (0.04)	580	0.61

Photophysical Properties

Absorption spectra

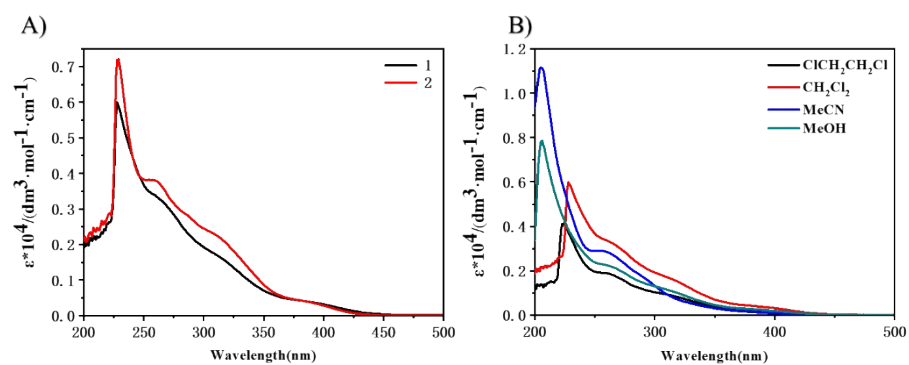


Fig. S6. Absorption spectra of **1** and **2** in CH_2Cl_2 (A), and **1** in different solutions (B).

Performance comparison

Table S4: Performance comparison of fabricated white LEDs with previously reported Cu-based white LEDs.

Component	CIE(x, y)	CCT	CRI	Efficiency (lm/W)	Reference
Cu ₁₄ DT ₁₀ and Au@DT	(0.32, 0.36)	/	/	/	6
Cu(0) ₄ Cu(I) ₁₀ DT ₁₀ and Au(0) ₁₁ Au(I) ₄ DT ₁₅	(0.31, 0.36)	6577	88	/	7
Cu@AA, VG61E and MPR635	(0.35, 0.33)	4742	92	9.8	8
Cu@GSH and Cu@AA	(0.36, 0.31)	4163	91	≈2.3	9
Cu@GSH /polyurethane film	(0.34, 0.29)	/	87	/	10
Au(I)-doped Cu@DT	(0.33, 0.41)	5289	86	/	11
MMI-CuNC and NAC-CuNC	(0.26, 0.30)	11038	83	/	12
[Cu ₃ (μ ₃ -H)(μ ₂ -dppy) ₄](ClO ₄) ₂	(0.33,0.31)	5281	83.7	41.32	This work

References

- 1 Y. J. Li, Z. Y. Deng, X. F. Xu, H. B. Wu, Z. X. Cao and Q. M. Wang, *Chemical communications*, 2011, **47**, 9179-9181.
- 2 Sheldrick, G. M. SHELXL-97, Program for the Refinement of Crystal Structures; University of Göttingen, Göttingen, Germany, 1997.
- 3 A. Gk and B. Jf, *Computational Materials Science*, 1996, **6**, 15-50.
- 4 G. Kresse and D. Joubert, *Physical Review B*, 1999, **59**, 1758-1775.
- 5 S. Grimme, J. Antony, S. Ehrlich and H. Krieg, *Journal of Chemical Physics*, 2010, **132**, 154104.
- 6 Z. Wu, J. Liu, Y. Gao, H. Liu, T. Li, H. Zou, Z. Wang, K. Zhang, Y. Wang, H. Zhang and B. Yang, *Journal of the American Chemical Society*, 2015, **137**, 12906-12913.
- 7 J. Liu, Z. Wu, T. Li, D. Zhou, K. Zhang, Y. Sheng, J. Cui, H. Zhang and B. Yang, *Nanoscale*, 2016, **8**, 395-402.
- 8 Z. Wang, A. S. Sussha, B. Chen, C. Reckmeier, O. Tomanec, R. Zboril, H. Zhong and A. L. Rogach, *Nanoscale*, 2016, **8**, 7197-7202.
- 9 Z. Wang, B. Chen, A. S. Sussha, W. Wang, C. J. Reckmeier, R. Chen, H. Zhong and A. L. Rogach, *Advanced science*, 2016, **3**, 1600182.
- 10 Z. Wang, B. Chen, M. Zhu, S. V. Kershaw, C. Zhi, H. Zhong and A. L. Rogach, *ACS applied materials & interfaces*, 2016, **8**, 33993-33998.
- 11 J. Liu, Z. Wu, Y. Tian, Y. Li, L. Ai, T. Li, H. Zou, Y. Liu, X. Zhang, H. Zhang and B. Yang, *ACS applied materials & interfaces*, 2017, **9**, 24899-24907.
- 12 H. H. Deng, Q. Q. Zhuang, K. Y. Huang, P. Balasubramanian, Z. Lin, H. P. Peng, X. H. Xia and W. Chen, *Nanoscale*, 2020, **12**, 15791-15799.